



<http://jaet.journals.ekb.eg>

# Enhancing Egyptian Kaolin Properties through Additive Engineering: Insights from Poly(vinyl alcohol), Silica Nanoparticles, and Activated Carbon

Nasser A. M. Barakat<sup>1,\*</sup>, Neama A. M. Eltohamy<sup>2</sup>, Wesam Elhawam<sup>3</sup> and Kasem R. M. Abdelrazek<sup>2</sup>

<sup>1</sup>Chemical Engineering Department, Faculty of Engineering, Minia University, Minia 61516, Egypt.

<sup>2</sup>Department of Holographic Expression, Faculty of Art Education, Minia University, Minia 61516, Egypt.

<sup>3</sup>Department of Holographic Expression, Faculty of Art Education, Helwan University, Cairo 11795, Egypt

Corresponding author Email: [nasbarakat@mu.edu.eg](mailto:nasbarakat@mu.edu.eg)

## Abstract

This study investigates the efficacy of poly(vinyl alcohol) (PVA), silica nanoparticles (SiO<sub>2</sub>), and activated carbon (AC) as additives for enhancing ceramic characteristics of the Egyptian kaolin. Through rigorous characterization, including plasticity, compression strength, water absorption, and porosity analysis, the impact of these additives on Egyptian kaolin performance is assessed. Poly(vinyl alcohol) was dissolved in the used water to form kaolin mud, while the additives were added to the polymer aqueous solution before adding the clay powder. Results reveal notable improvements in key mechanical parameters with the incorporation of PVA, wherein plasticity increased by up to 22.8% and compression strength reached 2.47 MPa. SiO<sub>2</sub> nanoparticles contribute to enhanced densification and reduced porosity, with a significant decrease observed in water absorption. Furthermore, the addition of activated carbon enhances the mechanical properties, contributing to improved mechanical integrity. Interestingly, it was found that addition the proposed materials leads to maintain the density throughout the sintering process as it was observed that trivial change in the apparent density between the samples sintered at 900 and 1050 °C. This finding strongly supports exploiting this kaolin as refractory ceramics in ovens and kilns. Overall, this study underscores the versatility of PVA, SiO<sub>2</sub>, and AC as effective additives for tailoring the properties of ceramic materials, offering promising avenues for applications in diverse industrial sectors.

**Keywords:** Egyptian kaolin; Poly(vinyl alcohol); Silica nanoparticles; Activated carbon; Additive engineering.

## 1. Introduction

Kaolin, a hydrated aluminum silicate predominantly composed of the mineral kaolinite, holds immense significance as an industrial clay mineral globally due to its versatile physical and chemical properties [1-4]. Particularly in the ceramics industry, kaolin finds widespread use in diverse applications ranging from dinnerware to refractories [5, 6].

Despite its industrial importance, the ceramics sector in Egypt faces challenges due to the inconsistent quality of local kaolin deposits, leading to a reliance on imported kaolin to meet approximately 73% of industry demands [7, 8]. This inconsistency often results in the production of waste materials due to non-compliance with required specifications for ceramic production. Therefore, the main aim of this work is improving the rheology and ceramic

characteristics of the Egyptian kaolin to widen its application in the ceramic industries.

Previous studies on Egyptian clays have primarily focused on mineralogical and chemical compositions, rheology, drying and firing characteristics, and whiteness [9, 10]. Notably, challenges such as high plasticity during shaping and the requirement for high densification temperatures hinder widespread application [11].

Traditionally, the addition of ball clay has been the primary strategy to enhance plasticity, albeit with limitations. However, leveraging the unique properties of nanomaterials presents a promising avenue for improving the characteristics of Egyptian kaolin. In this context, our study explores novel strategies aimed at enhancing the properties of Egyptian kaolin through the incorporation of poly(vinyl alcohol) (PVA), silica nanoparticles (SiO<sub>2</sub>), and activated carbon (AC) [12, 13].

Revised:7 April , 2024, Accepted:12 June , 2024

We specifically investigate the efficacy of these additives in improving plasticity, apparent density, compression strength, water absorption, and surface porosity. The selection of additives is deliberate, allowing us to discern the influence of additive nature (carbonaceous or metal oxides) and nanostructure morphology (long and short axial ratios) on the resultant characteristics of kaolin products.

Our findings underscore the profound impact of these additives on enhancing the properties of Egyptian kaolin, offering new possibilities for advanced ceramic applications. Through this manuscript, we aim to contribute to the ongoing discourse on optimizing industrial clay minerals, particularly Egyptian kaolin, for enhanced utility in ceramic production, thereby fostering innovation and sustainability in materials engineering.

## 2. Experimental work

### 2.1 Materials

Egyptian kaolin has been obtained from the local market in Aswan city. Table 01 shows the chemical composition of the used kaolin. The kaolin was crushed, grinded and sieved to pass the 200 ASTM mesh sieve.

**Table 01: Chemical composition (%) of the Egyptian clay[14].**

SiO <sub>2</sub>	TiO <sub>2</sub>	Al <sub>2</sub> O <sub>3</sub>	Fe <sub>2</sub> O <sub>3</sub>	MnO	MgO	CaO	Na <sub>2</sub> O	K <sub>2</sub> O	P <sub>2</sub> O <sub>5</sub>
45-50	1-2	32-38	0.2-0.7	0.0-0.02	0.0-0.3	0.0-0.5	0.0-0.05	0.0-0.1	0.0-0.1

Poly (vinyl alcohol) (PVA, M.wt.79000, Alfa Aesar), was used as received. Activated carbon was obtained from Eisen-Golden Laboratories.

### 2.2 Silicon oxide nanoparticles

The process of synthesizing silica nanoparticles from rice husk involves several steps, starting with the rinsing of RH in alcohol and deionized water to remove impurities and contaminants. Subsequently, the dried RH is crushed, ground, and sieved to achieve uniform particle size (70–75 μm), ensuring homogeneity in the resulting silica nanoparticles. Calcination of the prepared RH under air at 700°C, with a heating rate of 3°C/min and a 2-hour holding time, leads to the decomposition of organic components present in RH, such as cellulose and

lignin, and the conversion of silica precursors into amorphous silica nanoparticles.

### 2.3 Functionalization of the activated carbon

The used activated carbon has hydrophobic property. Therefore, to get homogeneous water slurry from these materials, functionalization process was performed by making a reflux treatment using sulfuric acid/nitric acid solution. In a clean and dry glass beaker, the required quantities of sulfuric acid and nitric acid in a ratio of 3:1 by mass were measured. The measured acids were added to the beaker, ensuring proper ventilation in a fume hood. The acid mixture was gently stirred using a glass stirring rod to ensure homogeneity. The desired quantity of activated carbon was measured and transferred into a clean round-bottom flask. The prepared acid solution to the flask containing the carbonaceous materials to have a 1 wt% slurry. The round-bottom flask equipped with a reflux condenser is placed onto a magnetic stirrer. The reflux apparatus was assembled carefully to ensure a tight seal between the flask and the condenser to prevent vapor escape. The reaction mixture was heated under reflux conditions to keep boiling for 1 hour. After the reflux treatment, the reaction mixture was allowed to cool to room temperature naturally. Once cooled, the contents of each flask were transferred to separate clean glass beakers. The acid-treated activated carbon was diluted with distilled water to neutralize the acidity. The suspension was filtered using a vacuum filtration setup with filter paper. The acid-treated carbonaceous materials were washed several times with distilled water to remove any residual acid. After washing, the produced materials were dried under vacuum at 60 °C for one night.

### 2.4 Experimental procedure

Each additive (0.08 g) was dispersed in 45 ml of water to create a slurry. Overall, the proposed additives were used along with PVA in all samples. To investigate the additive content, three groups of samples were prepared. For the first group of samples (coded by -1), 10 ml of the additive slurry was combined with 35 ml of PVA aqueous solution containing 1 g PVA to obtain the required 45 ml slurry for making the kaolin mud. For the second group of samples (coded by -2), 15 ml of the slurry was mixed with 30 ml of PVA aqueous solution containing 1 g PVA. While in the third group of

samples (coded by -3), 20 ml of the slurry was mixed with 25 ml of PVA aqueous solution containing 1 g PVA. Each prepared PVA/additive slurry was used to form mud with 150 g of Kaolin powder. The mud mixture was thoroughly mixed until homogeneity was achieved. The homogenized mud was molded into cubes with dimensions of 2×2×2 cm<sup>3</sup>. The formed cubes were dried in an oven at 100°C for 24 hours to remove any residual moisture. Subsequently, the dried cubes were subjected to calcination at two different temperatures: 900°C and 1050°C. Then, the cubes became ready for the characterization process. The experimental procedure was replicated for each group of samples to ensure consistency and reliability of results. Control samples without additives were also prepared following the same procedure for comparison purposes.

### 2.5 Characterizations

The produced materials underwent comprehensive characterization at the Central Laboratory for Microanalysis and Nanotechnology, Minia University. The morphological features of the materials were investigated using scanning electron microscopy (SEM) with a Hitachi S-7400 scanning electron microscope from Japan. For comprehensive analysis of the chemical composition, X-ray diffraction (XRD) was performed using a Rigaku X-ray diffractometer from Tokyo, Japan.

To measure the apparent density, water absorption and the surface porosity, the pristine and modified of clay cubes, the weight of the dry sample ( $W_D$ ) was estimated then the cube was soaked in water for 30 min, then the weight of the soaked cubes ( $W_S$ ) has been estimated. After removing from water, the excess water around the cubes has been removed by cleaning tissue, then the weight of the cleaned cubes ( $W_C$ ) was estimated. Later, the following equations were used to estimate the properties:

$$\text{Apparent density} = \frac{W_D}{W_C - W_S} \text{ g/cm}^3 \quad (1)$$

$$\text{Water absorption} = \frac{W_C - W_D}{W_D} \times 100 \quad (2)$$

$$\text{Apparent porosity} = \frac{W_C - W_D}{W_C - W_S} \times 100 \quad (3)$$

The plasticity was measured by shaping rods from various mud samples formed by adding different amounts of water (or additive slurry) to the kaolin powder, the rod diameter was kept at 3.25 mm. Water

(or slurry) content was decreased until appearing cracks on the rod. Then, the rod was subjected to drying at 110 °C for 24 h to estimate the exact weight of water in the cracked rod. Then the plasticity is calculated from this equation [15]:

$$\text{Water absorption} = \frac{\text{Exact water weight in the cracked rod}}{\text{Weight of the dry rod}} \times 100 \quad (4)$$

The experiment has been repeated three times and the average value was used.

ASTM C109 compression test has been achieved to investigate the mechanical properties using Tinius Olsen (H5KT model) Benchtop Tester (USA).

The samples were prepared by the following procedure. First, PVA aqueous solution was prepared by dissolving 1 g of the polymer granules in 45 mL water. Slurries from the inorganic additives have been prepared by adding 0.08 g from the solid material to 45 mL distilled water, the mixture was subjected to ultrasonication treatment for 30 min to have complete dispersion. Several samples were prepared and coded in table 1. In each sample, 150 g of fine Egyptian kaolin was mixed with 45 ml blend from PVA aqueous solution and the additives slurry according to table 1. After formation of homogeneous mud, a 2×2×2 cm cube was formed, dried, and sintered at different temperatures.

**Table 1 Composition of the prepared samples**

Code	PVA aqueous solution (mL)	SiO <sub>2</sub> slurry (mL)	AC slurry (mL)
PVA	45	--	--
SiO2-1	35	10	--
SiO2-2	30	15	--
SiO2-3	25	20	--
AC-1	35	--	10
AC-2	30	--	15
AC-3	25	--	20

For comparison, a pristine kaolin sample was prepared (coded kaolin) by mixing 150 g of kaolin powder with 45 mL distilled water.

### 3. Results and discussion

### 3.1 Additives characteristics

The SEM images displayed in Fig. 1 showcase the morphology of the synthesized silicon oxide (silica) nanoparticles obtained from the calcination of rice husk (RH). The images reveal nanoparticles with a random morphology and a wide range of sizes, indicating the successful transformation of RH into silica nanoparticles through the calcination process [16]. The utilization of rice husk as a precursor for silica nanoparticles offers several advantages, making it an attractive and sustainable option for nanoparticle synthesis. Rice husk, an agricultural waste product, is abundantly available and renewable, making it a cost-effective and environmentally friendly precursor for silica nanoparticles synthesis. The controlled calcination conditions are crucial for achieving desired properties and morphology in the synthesized silica nanoparticles [17].

The random morphology observed in the SEM images reflects the heterogeneous nature of the precursor material and the complex structure of rice husk. The varying sizes of the nanoparticles can be attributed to differences in the distribution and composition of silica precursors within the RH matrix, as well as the calcination process parameters [18].

Furthermore, the synthesis of silica nanoparticles from rice husk offers potential applications in various fields, including catalysis, drug delivery, sensors, and environmental remediation. The unique properties of silica nanoparticles, such as high surface area, tunable porosity, and biocompatibility, make them promising candidates for diverse applications.

The X-ray diffraction (XRD) pattern presented in Fig. 2 reveals distinctive peaks at specific  $2\theta$  values, which are indicative of the crystallographic structure of the produced silicon dioxide ( $\text{SiO}_2$ ) nanoparticles. As shown in the obtained pattern, the prepared  $\text{SiO}_2$  NPs shows wider and comparatively lower intensity peaks. This observation suggests that the synthesized  $\text{SiO}_2$  nanoparticles may possess an amorphous or partially crystalline structure.

The broadening and reduced Intensity of the XRD peaks pattern can be attributed to several factors, including the amorphous nature of the nanoparticles and the presence of structural defects or disorder. Amorphous materials lack long-range order in their atomic arrangement, resulting in diffuse scattering of X-rays and broader peaks in the XRD pattern.

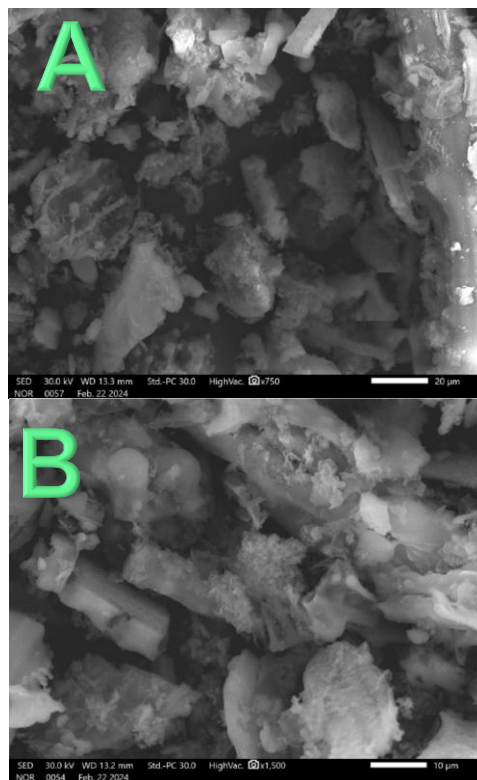


**Fig. 1 Two magnifications SEM images for the produced  $\text{SiO}_2$  nanoparticles**

Additionally, the presence of crystalline imperfections or grain boundaries can contribute to peak broadening and reduced intensity. Another possible reason for the observed XRD pattern characteristics could be the presence of nanoscale crystallites or nanodomains within the  $\text{SiO}_2$  nanoparticles. Nanosized crystallites can lead to peak broadening due to size effects, such as strain and finite size contributions, resulting in lower intensity and wider peaks in the XRD pattern [19]. The synthesis conditions and processing parameters employed during the preparation of  $\text{SiO}_2$  nanoparticles can also influence their crystallinity and XRD pattern characteristics. For instance, variations in calcination temperature, heating rate, and duration can impact the degree of crystallinity and structural ordering in the synthesized nanoparticles [20].

The SEM images displayed in Fig. 3 depict the treated activated carbon, revealing a heterogeneous distribution of particles with varying sizes and non-uniform shapes. This characteristic suggests a high

surface area and a propensity for interconnection with the kaolin powder, which holds significant implications for enhancing the mechanical properties of ceramic materials.

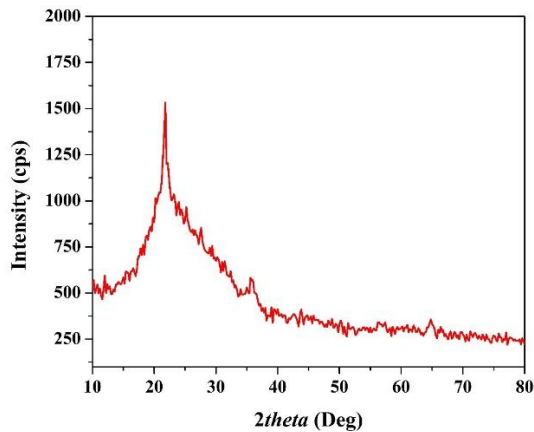


**Fig. 2 XRD pattern for the prepared silicon oxide.**

The irregular particle shape and high surface area of activated carbon might facilitate strong interfacial bonding with the kaolin matrix. This reinforcement mechanism helps to improve the mechanical integrity of the ceramic composite, leading to enhanced strength and toughness. Moreover, the interconnected network of activated carbon particles within the ceramic matrix can act as a barrier to crack propagation. This impediment to crack growth enhances the material's toughness, making it more resistant to fracture and impact damage. Furthermore, activated carbon particles can fill voids and pores within the ceramic structure, thereby reducing porosity. Lower porosity enhances the material's density and homogeneity, resulting in improved mechanical properties such as compression strength and hardness. The presence of activated carbon can enhance the wear resistance of ceramic materials by providing additional reinforcement against abrasive forces. This can prolong the service life of ceramic components subjected to frictional wear in various applications. Overall, the properties of activated carbon, such as particle size, surface chemistry, and porosity, can be tailored through various treatment methods. This allows for the customization of ceramic composites with desired mechanical properties to meet specific application requirements.

### 3.2 Characterizations of the modified kaolin

#### 3.2.1 Plasticity limit.

The plasticity of kaolin mud is a crucial factor in its shaping process, as it determines the ability of the mud to be molded into desired forms without cracking or deforming. Low plasticity limit in Egyptian kaolin mud has been identified as a significant challenge in ceramic production. Fig. 4 illustrates the plasticity enhancement achieved by incorporating proposed additives into the kaolin mud, addressing this issue.

The measured plasticity of pristine kaolin mud was found to be 13.122%. However, the utilization of proposed additives led to notable improvements in plasticity, with values ranging from 19.2368% to 22.8284%. These results signify the effectiveness of the additives in enhancing the plasticity of the kaolin mud, thereby improving its suitability for shaping and forming processes in ceramic production.

The plasticity enhancement achieved in kaolin mud with the incorporation of  $\text{SiO}_2$  and activated carbon (AC), along with polyvinyl alcohol (PVA), was investigated across three different concentrations (low; code -1, medium; code -2, and high; code -3). PVA, utilized in conjunction with all additives, acts as a binder and plasticizer, enhancing the interparticle interactions and facilitating better dispersion of other additives within the kaolin matrix. The addition of PVA contributes to increased plasticity by promoting better cohesion and fluidity of the kaolin mud, leading to improved shaping, and forming characteristics.

$\text{SiO}_2$  nanoparticles, when combined with PVA, effectively improve plasticity by acting as lubricants between kaolin particles. At low concentrations ( $\text{SiO}_2$ -1), the lubricating effect of  $\text{SiO}_2$  nanoparticles is moderate, resulting in a modest increase in plasticity. Medium ( $\text{SiO}_2$ -2) concentration of  $\text{SiO}_2$  nanoparticles further enhance plasticity by reducing friction and facilitating smoother particle movement within the mud matrix. However, more increase in the concentration ( $\text{SiO}_2$ -3) showed relatively negative impact which could be attributed to start formation of barrier layers between the clay particles.

The observed trend in plasticity enhancement with the incorporation of activated carbon (AC) in kaolin mud, in conjunction with polyvinyl alcohol (PVA), reveals interesting insights into the role of AC concentration on plasticity improvement. The results

indicate that while a small amount of AC (AC-1 sample) led to a slight decrease in plasticity compared to PVA only, increasing the AC content resulted in significant improvements in plasticity.

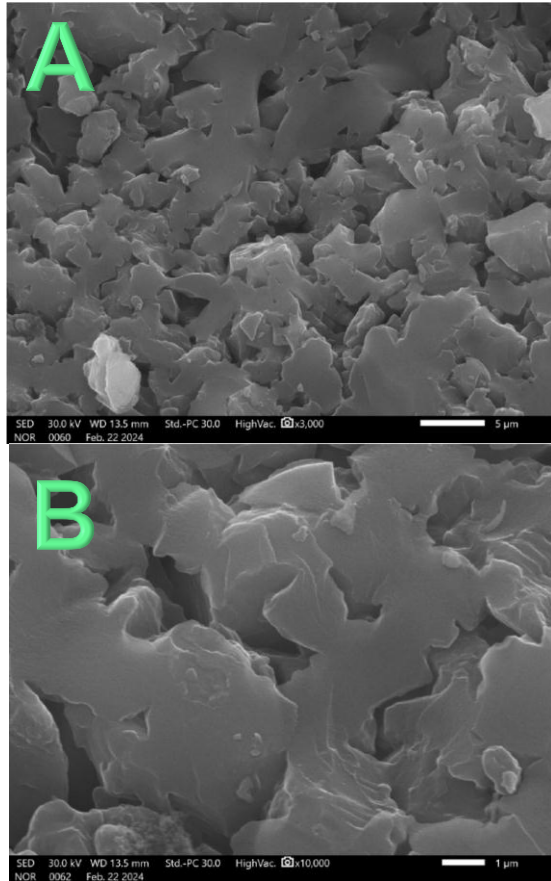


**Fig. 3 Two magnifications SEM images for the treated activated carbon.**

The slight decrease in plasticity observed in the AC-1 sample compared to the PVA-only sample may be attributed to the initial interaction between AC particles and the kaolin matrix. The presence of a small amount of AC may slightly disrupt the rheological properties of the kaolin mud, resulting in decreased flowability and moldability.

In contrast, increasing the AC content in the AC-2 and AC-3 samples resulted in notable improvements in plasticity compared to the PVA-only sample. At medium and high concentrations, AC particles are more effectively dispersed within the mud matrix, leading to enhanced particle interaction and lubrication between kaolin particles. The increased surface area and porosity of AC at higher concentrations contribute to better water retention

and rheological properties of the mud, thereby improving plasticity. Additionally, the presence of AC may act as a reinforcing agent, enhancing the mechanical stability of the mud matrix and reducing cracking during shaping processes.

These findings highlight the importance of optimizing AC concentration to achieve the desired plasticity enhancement in kaolin-based materials. By carefully adjusting the AC dosage, it is possible to tailor the rheological properties of kaolin mud for specific applications in ceramic production and other industrial sectors.

The observed variation in plasticity enhancement among different additives and concentration levels underscores the importance of optimizing additive composition and dosage for achieving desired performance characteristics in kaolin mud. By understanding the synergistic effects of additives and their interactions with the kaolin matrix, it is possible to tailor the plasticity and rheological properties of kaolin-based materials for specific applications in ceramic production and other industrial sectors.

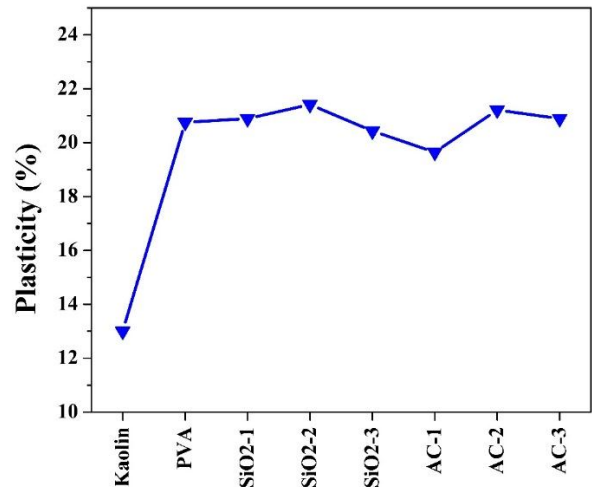


**Fig. 4 Plasticity limit (%) for pristine and modified Egyptian kaolin**

### 3.2.2 Compression strength

The compression strength measurements provide valuable insights into the mechanical properties of the pristine and modified kaolin samples, shedding light on the effectiveness of various additives in enhancing the strength characteristics. The samples have been sintered at two temperatures: 900 and 1050 °C.

### 3.2.2.1 At 900 °C:

As shown in Fig. 5, the observed trends in compression strength, compared to the pristine kaolin and PVA-only samples, reveal the complex interplay between additive type, concentration, and resulting material properties. PVA, when used alone, significantly increases the compression strength of kaolin samples (2.075 MPa) compared to the pristine kaolin (1.7275 MPa). This improvement can be attributed to the binding and strengthening properties of PVA, which enhance the cohesion and integrity of the kaolin matrix. However, different effects of the other additives have been observed as follows:

Incorporating SiO<sub>2</sub> nanoparticles, in conjunction with PVA, resulted in a decrease in compression strength compared to the pristine kaolin. This reduction may be attributed to the dispersing effect of SiO<sub>2</sub> nanoparticles, which may compromise the structural integrity of the kaolin matrix at certain concentrations. However, the observed decrease in compression strength with SiO<sub>2</sub> incorporation contrasts with the trend observed with other additives, such as activated carbon (AC), suggesting unique interaction mechanisms between SiO<sub>2</sub> nanoparticles and the kaolin matrix. Numerically for the low, moderate, and high concentrations, SiO<sub>2</sub>-1, SiO<sub>2</sub>-2 and SiO<sub>2</sub>-3, the observed compression strength was 1.56, 1.558 and 1.425 MPa, respectively.

At low and moderate concentrations, the compression strength of AC-based samples was lower compared to the pristine kaolin, indicating a potential weakening effect of AC on the kaolin matrix at these concentrations. However, increasing the AC content led to an improvement in compression strength, surpassing that of the pristine kaolin at high concentrations. This improvement may be attributed to the reinforcing effect of AC, which enhances the mechanical stability and integrity of the kaolin matrix.

### 3.2.2.2 At 1050 °C:

The compression strength measurements conducted at a higher sintering temperature of 1050°C provide valuable insights into the mechanical behavior of the pristine and modified kaolin samples. These results reveal notable enhancements in compression strength compared to those observed at the lower sintering temperature of 900°C. The pristine kaolin exhibits a

significant increase in compression strength, reaching 2.07 MPa at 1050°C, representing a notable improvement of 19.8% compared to the strength observed at 900°C. This enhancement can be attributed to the increased densification and crystallization of the kaolin matrix at higher temperatures, resulting in improved mechanical properties. Similarly, the compression strength of the PVA-modified kaolin sample also increases to 2.345 MPa at 1050°C, representing a considerable improvement of around 13% compared to the strength observed at 900°C. This increase is consistent with the densification and strengthening effects associated with higher sintering temperatures. The SiO<sub>2</sub> nanoparticle-modified kaolin samples exhibit remarkable improvements in compression strength upon increasing the sintering temperature from 900°C to 1050°C.

- At the highest SiO<sub>2</sub> concentration (SiO<sub>2</sub>-3), the compression strength increases by approximately 53%, from 1.45 MPa at 900°C to 2.18 MPa at 1050°C. This substantial improvement underscores the synergistic effects of SiO<sub>2</sub> nanoparticles and higher sintering temperatures in enhancing the mechanical properties of the kaolin matrix.
- Similarly, the moderate SiO<sub>2</sub> concentration (SiO<sub>2</sub>-2) shows a significant increase in compression strength, with a 42.4% improvement from 1.56 MPa at 900°C to 2.25 MPa at 1050°C. This enhancement highlights the effectiveness of SiO<sub>2</sub> nanoparticles in promoting densification and strengthening mechanisms at elevated temperatures.
- In contrast, the lowest SiO<sub>2</sub> concentration (SiO<sub>2</sub>-1) exhibits a relatively modest improvement of only 13.3% in compression strength upon increasing the sintering temperature. This result suggests that the reinforcing effects of SiO<sub>2</sub> nanoparticles may be less pronounced at lower concentrations, limiting the extent of improvement in mechanical properties [21].

The observed variations in compression strength among the activated carbon (AC)-based samples, particularly in response to different concentrations and sintering temperatures, offer valuable insights into the complex interplay between AC content,

sintering conditions, and resulting material properties.

- Increasing the sintering temperature from 900°C to 1050°C resulted in varying degrees of improvement in compression strength across the AC-based samples.
- For the low AC concentration sample (AC-1), the compression strength significantly improved by 38.4% when the sintering temperature was increased to 1050°C. This enhancement can be attributed to the increased densification and crystallization of the kaolin matrix at higher temperatures, leading to improved mechanical properties.
- However, the magnitude of improvement in compression strength upon increasing the sintering temperature decreased with increasing AC content. Specifically, while the moderate concentration sample (AC-2) still exhibited a 14.7% improvement, further increases in AC content (AC-3) led to a decrease in compression strength at the higher sintering temperature.
- The observed decrease in compression strength for the AC-3 sample at 1050°C suggests that excessive AC content may have adverse effects on the structural integrity and mechanical properties of the kaolin matrix, potentially due to aggregation or inadequate dispersion of AC particles [22].

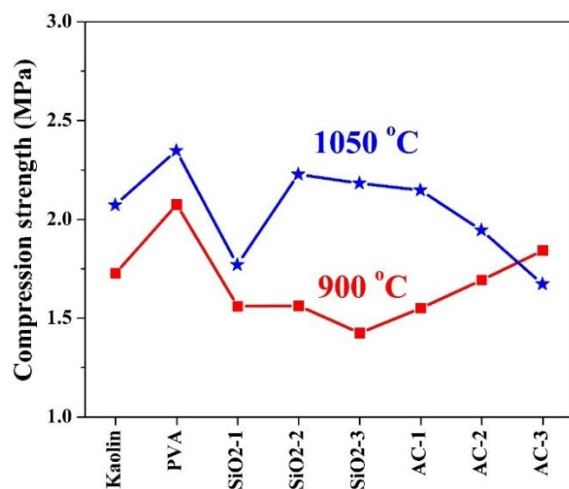


**Fig. 5 Compression strength of pristine and modified Egyptian kaolin sintered at two temperatures: 900 and 1050 °C.**

### 3.2.3 Apparent density

The observed changes in the apparent density of the pristine and modified kaolin samples after sintering at different temperatures, in Fig. 6, provide valuable insights into the effects of additives and sintering conditions on the densification behavior of the kaolin matrix.

At the lower sintering temperature of 900°C, minimal changes in the apparent density of the kaolin samples were observed, regardless of the additives used. This suggests that the densification of the kaolin matrix was limited at this temperature, resulting in negligible alterations in apparent density. However, upon increasing the sintering temperature to 1050°C, a significant decrease in the apparent density of the pristine kaolin was observed, with a reduction of approximately 9%. This decrease can be attributed to enhanced densification and consolidation of the kaolin particles at higher temperatures, leading to a reduction in pore volume and thus lower apparent density. The decrease in apparent density of the pristine kaolin at 1050°C can be also attributed to the increased diffusion and rearrangement of particles, leading to more efficient packing and reduced pore volume within the matrix.

Interestingly, for the additives investigated, no considerable decrease in apparent density was observed at the higher sintering temperature of 1050°C at all concentrations. This suggests that the additives did not significantly affect the densification behavior of the kaolin matrix under the tested conditions. The consistent apparent density values across different additive-modified samples at 1050°C indicate that the presence of additives did not impede the densification process, nor did they introduce additional porosity or voids within the kaolin matrix during sintering.

The lack of significant changes in apparent density with the addition of additives suggests that these materials did not hinder the densification process. Instead, they may have contributed to improved particle packing or promoted sintering mechanisms, such as grain boundary diffusion, resulting in denser microstructures [23]. Additionally, the interaction between additives and kaolin particles may have facilitated the formation of stronger interfacial bonds or secondary phases, which could have further contributed to densification without compromising apparent density [24].



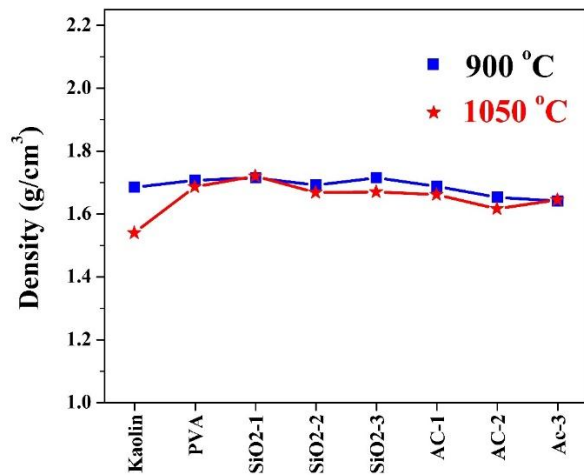


**Fig. 6 Apparent density of pristine and modified Egyptian kaolin sintered at two temperatures: 900 and 1050 °C.**

### 3.2.4 Water absorption

The water absorption results depicted in Fig. 7 provide valuable insights into the effects of additives and sintering temperature on the porosity and moisture uptake behavior of kaolin-based ceramics. The addition of PVA resulted in a significant reduction in water absorption for both sintering temperatures (900°C and 1050°C), indicating improved densification and reduced porosity in the kaolin matrix. PVA, being a polymeric binder, can act as a sintering aid and promote particle packing, leading to enhanced compaction and reduced pore volume during firing. The observed decrease in water absorption with PVA addition highlights its effectiveness in improving the impermeability and moisture resistance of the ceramic material, making it suitable for applications requiring low water absorption, such as in sanitaryware or tiles.

In contrast to PVA, the other additives used in conjunction showed minimal impact on water absorption, particularly at 900°C sintering temperature. This trivial effect on water absorption suggests that these additives may not significantly alter the microstructure or porosity of the kaolin matrix under the tested conditions. The lack of substantial reduction in water absorption with these additives may be attributed to factors such as inadequate dispersion, weak interaction with the kaolin particles, or limited sintering promotion capabilities compared to PVA.

The slight increase in water absorption observed for some additives at 1050°C, such as SiO2-2, and AC-1, may be attributed to factors such as phase transformations, secondary phase formation, or incomplete densification at higher temperatures.

Interestingly, increasing the sintering temperature from 900°C to 1050°C did not lead to a significant change in water absorption for all samples, indicating that the effects of sintering temperature on porosity reduction were limited. This observation suggests that the sintering conditions employed may have already achieved near-optimal densification at 900°C, with further increases in temperature providing marginal improvements in pore closure or compaction.

The findings underscore the importance of PVA as an effective additive for reducing water absorption in kaolin-based ceramics, highlighting its potential for enhancing moisture resistance and durability in various applications.

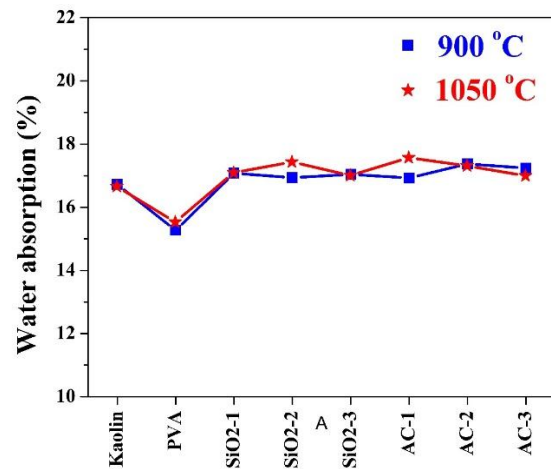


**Fig. 7 Water absorption of pristine and modified Egyptian kaolin sintered at two temperatures: 900 and 1050 °C.**

### 3.2.5 Porosity

The porosity results presented in Fig. 8 provide valuable insights into the effects of additives and sintering temperature on the pore structure and density of kaolin-based ceramics. These findings complement the water absorption results discussed earlier, highlighting the relationship between porosity and water absorption characteristics.

Consistent with the water absorption findings, addition of PVA led to a significant reduction in porosity for both sintering temperatures (900°C and

1050°C). This reduction in porosity corresponds to the decreased water absorption observed in the PVA-modified samples. The denser microstructure achieved with PVA contributes to lower water absorption due to reduced accessibility of water into the pores.

In contrast to PVA, the other additives used alongside showed minimal influence on porosity reduction, particularly evident at 900°C sintering temperature. This finding aligns with the trivial impact of these additives on water absorption, indicating a lack of significant alteration in pore structure. The minimal changes in porosity with these additives suggest that their effects on water absorption are closely linked to the density and distribution of pores within the ceramic matrix.

At 1050°C sintering temperature, most additives exhibited an opposite influence on porosity compared to PVA, resulting in increased porosity relative to pristine kaolin. This corresponds to the observed increase in water absorption with certain additives at this temperature. The increase in porosity with these additives may be attributed to factors such as phase transformations, secondary phase formation, or incomplete densification, which could introduce additional pores or defects within the ceramic matrix. Increasing the sintering temperature from 900°C to 1050°C did not significantly alter the porosity of the samples. This observation is consistent with the minimal changes in water absorption across different sintering temperatures, indicating limited effects on pore closure or compaction.

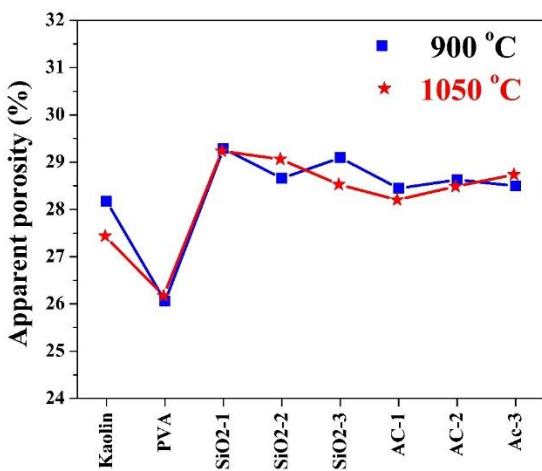


**Fig. 8 Porosity of pristine and modified Egyptian kaolin sintered at two temperatures: 900 and 1050 °C.**

#### 4. Conclusions

In conclusion, this study comprehensively investigated the effects of poly(vinyl alcohol), silica nanoparticles, and activated carbon additives on ceramic materials. Through rigorous characterization, including plasticity, compression strength, water absorption, and porosity analysis, significant insights were gained into the role of these additives in enhancing the mechanical and structural properties of ceramics. PVA demonstrated remarkable potential as a reinforcing agent, leading to a substantial increase in plasticity. SiO<sub>2</sub> nanoparticles contributed to densification and reduced porosity, while AC additives enhanced the mechanical properties, resulting in improved compression strength. Further research exploring optimization strategies and synergistic effects between additives could further advance the development of high-performance ceramic materials with tailored properties for specific applications. Overall, beside opening a new avenue to utilize the Egyptian kaolin in manufacturing the ceramic products, this study creates an additional usage for the Egyptian kaolin in refractory industry.

#### References

- [1] H.H. Murray, in: H.H. Murray (Ed.), *Developments in Clay Science*, Elsevier, 2006, pp. 85-109.
- [2] H.H. Murray, *Applied clay science*. 17 (2000) 207-221.
- [3] A. Anam, N. Gamit, V. Prajapati, B.Z. Dholakiya, *Materials Today Communications*. 36 (2023) 106827.
- [4] M.S. Shamsudin, A.T.M. Din, L. Sellaoui, M. Badawi, A. Bonilla-Petriciolet, S. Ismail, *Chem. Eng. J.* 465 (2023) 142833.
- [5] S.K. Hubadillah, M.H.D. Othman, T. Matsuura, A. Ismail, M.A. Rahman, Z. Harun, J. Jaafar, M. Nomura, *Ceram. Int.* 44 (2018) 4538-4560.
- [6] W.E. Worrall, *Ceramic Raw Materials: Institute of Ceramics Textbook Series*, Elsevier, 2013.
- [7] I. Bakr, *Applied clay science*. 52 (2011) 333-337.
- [8] N.A. Abdel-Khalek, *Applied Clay Science*. 15 (1999) 325-336.

- [9] O. Hegab, M. Serry, M. Kora, M. Abu Shabana, Proceedings of the Symp held jointly with the Egyptian Geological Survey and Mining Projects Authority, 1992, p. 85p.
- [10] H.K. Sharaka, H.M. El-Desoky, M.W. Abd El Moghny, N.A.A. Hafez, S.A. Saad, Journal of Asian Earth Sciences: X. 7 (2022) 100087.
- [11] A. Muththalib, B.A. Baudet, ISSMGE, 2019.
- [12] H. Whittaker, J. Am. Ceram. Soc. 22 (1939) 16-23.
- [13] L.E. Jenks, The Journal of Physical Chemistry. 33 (2002) 1733-1757.
- [14] M.M. Elghandor, Research Journal Specific Education. 43 (2016) 1-7.
- [15] S.A.a.A.S. Afrah Kazem, Journal of the College of Basic Education for Educational and Human Sciences. 41 (2018) 1843-1850.
- [16] H. Chang, S.-Q. Sun, Chinese Physics B. 23 (2014) 088102.
- [17] S.D. Karande, S.A. Jadhav, H.B. Garud, V.A. Kalantre, S.H. Burungale, P.S. Patil, Nanotechnology for Environmental Engineering. 6 (2021) 29.
- [18] A. Shahbaz, M. Ayaz, U. Bin Khalid, L. Liaqat, Energy Sources, Part A: Recovery, Utilization, and Environmental Effects. 45 (2023) 1464-1484.
- [19] B.E. Warren, X-ray Diffraction, Courier Corporation, 1990.
- [20] Y. Jin, A. Li, S.G. Hazelton, S. Liang, C.L. John, P.D. Selid, D.T. Pierce, J.X. Zhao, Coord. Chem. Rev. 253 (2009) 2998-3014.
- [21] W. Li, K. Lu, J.Y. Walz, J. Am. Ceram. Soc. 95 (2012) 883-891.
- [22] S. Mopoung, N. Sriprang, J. Namahoot, Applied Clay Science. 88 (2014) 123-128.
- [23] E. Kłosek-Wawrzyn, J. Małolepszy, P. Murzyn, Procedia Engineering. 57 (2013) 572-582.
- [24] J. Lemaitre, B. Delmon, Journal of Materials Science. 12 (1977) 2056-2064.